

# Epsilon-Zero Resonance Antennas with Modified Unit Cells

Mohammad Saeed Majedi and Amir Reza Attari

**Abstract:** In this paper new epsilon-zero resonance (EZR) antennas using epsilon negative (ENG) transmission line (TL) are presented. In the proposed antennas, the unit cell of the ENG TL is implemented using a modified mushroom-like structure in which the via hole is placed at the patch edge. This configuration leads to a broadside radiation pattern and also results in the unit cell size reduction. A one unit cell compact size antenna and a nine unit cell high gain antenna using this new configuration are designed and fabricated. Measurement results including radiation pattern, maximum gain and return loss show good agreement with simulation results.

**Keywords:** Antenna, epsilon negative (ENG), epsilon zero resonance (EZR), metamaterials, zeroth order resonator (ZOR).

## 1. Introduction

Transmission line based metamaterials are effectively homogenous structures which were first presented in [1]-[3]. One of the unique applications of these artificial transmission lines is realization of the zeroth order resonators (ZORs) and using them as antenna [4]. The resonant frequency of this resonator is independent of the structure length, so it can be used to design either a compact size antenna or a large size one for higher gain applications.

The ZOR was first implemented using composite right/left handed (CRLH) transmission lines [4]-[6]. In addition to the CRLH TL, there are two other transmission line based metamaterials which can also be used as a ZOR. These are including epsilon negative (ENG) TL, introduced in [7] and [8], and mu negative (MNG) TL, introduced in [9]. The effective permittivity of ENG TL and effective permeability of MNG TL at their zeroth order resonant frequency are zero. Up to now many studies have been carried out about ZOR based antennas. These antennas are realized by using the CRLH TL [5], [6], [8], [10]-[14], ENG TL [7], [8], [15], [16] or MNG TL structures [9], [17]. In this paper, which is mainly based on the previous works presented in [7] and [8], a new configuration of ENG TL based ZOR is used to realize an EZR antenna. The unit cell of this new configuration is a modified mushroom-like structure in which the via hole is placed at one side of the patch. This structure provides a broadside radiation pattern, while the presented EZR antennas in [7] and [8] have non-broadside radiation characteristics. In addition, the proposed unit cell of the ENG TL has more compact size in comparison with the conventional ENG TL unit cells.

Based on this new structure, two antennas are designed and fabricated. One of them is constituted of one unit cell and has a compact size, while the other includes nine unit cells and hence it provides higher gain. Measurement results are presented for both antennas and compared with the simulation data.

## 2. One Unit Cell EZR Antenna

### 2.1 ENG TL Based ZOR

Figure 1 shows the equivalent circuit of an ENG TL which constitutes of N unit cells. The unit cell in this TL is including a series inductance,  $L_R$ , a shunt capacitance,  $C_R$ , and a shunt inductance,  $L_L$ . The zeroth order resonant frequency corresponds to the frequency that the electrical length,  $\theta = \beta\ell = \beta Np$ , is zero, where  $\beta$  is the phase constant of the ENG TL,  $\ell$  is the total length of it and  $p$  is the length of one unit cell. The zeroth order resonant frequency of an ENG resonator is determined by Eq. (1) [7]

$$f_0 = \frac{1}{2\pi\sqrt{L_L C_R}} \quad (1)$$

which is independent of the resonator length. It is easy to show that this resonant frequency is supported only when the ENG TL is open-ended [7].

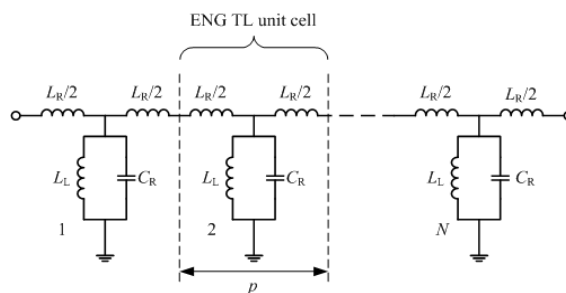


Fig. 1. Equivalent circuit of a N unit cell ENG TL.

### 2.2 Antenna Design

A common way for implementation of the ENG TL unit cell is using the mushroom-like structure. In fact the equivalent circuit of this structure is similar to the one unit cell of the ENG TL shown in Fig. 1. As an antenna and at the zeroth order resonant frequency, an in-phase electric field beneath this structure is made. Using equivalence theorem, a horizontal magnetic loop current is formed and this leads to a monopolar radiation pattern.

In this paper also we use the mushroom-like structure; however we change the structure in order to have a broadside radiation. Fig. 2 shows the top and side view of the proposed one unit cell EZR antenna which is fed at the centre of the patch. For realization of this antenna, the RF

Taconic-35 substrate with  $\epsilon_r = 3.5$ ,  $h = 1.524$  mm and  $\tan\delta = 0.0018$  has been used. As can be seen the structure of this antenna is mushroom-like but the via hole is placed at the one side of the patch. It will be shown later that this configuration leads to a broadside radiation pattern. In order to minimize the overall size of antenna, we used a coaxial line as the feed line. A capacitive slot ring with proper diameter around the feed point on the patch is used for antenna matching. By using this internal matching technique, there isn't need to use an external matching network and hence the overall size of antenna remains compact. More study on this matching mechanism will be presented in next sub-section.

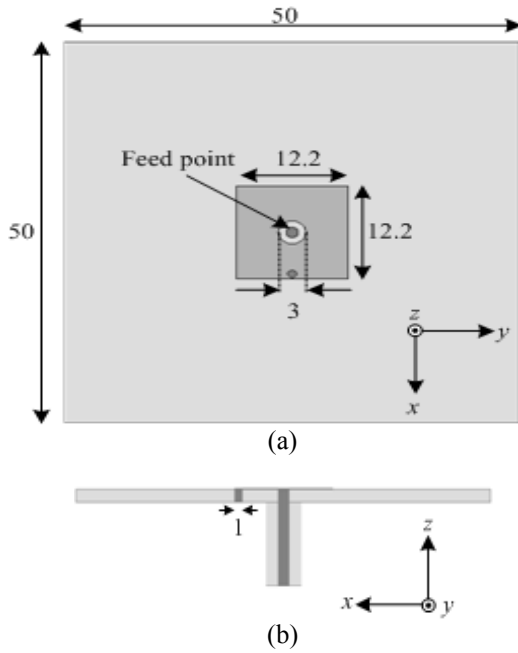


Fig. 2. Proposed one unit cell EZR antenna (a) Top view (b) Side view (dimensions are in millimetres).

Figure 3 illustrates the equivalent circuit of the proposed antenna. This equivalent circuit is similar to that of one unit cell of the ENG TL shown in Fig. 1. The shunt capacitance,  $C_R$ , is formed between the patch and the ground plane. The shunt inductance,  $L_L$ , results from the current flow on the patch in the x-direction along with the current flow in the via hole. The current flow on the patch in the y-direction also forms the series inductance of  $L_R$ . Finally  $C_m$  and  $G$  model the capacitive slot ring around the feed point and the radiation conductance, respectively.

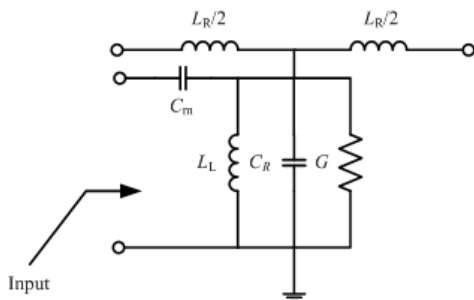


Fig. 3. Equivalent circuit of the proposed one unit cell EZR antenna.

For conventional mushroom-like structures, the shunt inductance,  $L_L$ , results only from the current flow in the via hole. Hence  $L_L$  in the modified mushroom-like structure has larger value which leads to a lower resonant frequency. In the other words, this new structure is more compact than the conventional one. It is worthy to mention that according to Fig. 3 there is no current in the series inductances. This means that the current flow on the patch is only in x-direction and there is no current in y-direction.

### 2.3 Antenna Matching

The presented antenna is simulated using HFSS software. Fig. 4 illustrates the input impedance of this antenna without capacitive ring. The resonant frequency is  $f_0 = 2.47$  GHz. According to Fig. 4, the input resistance of the antenna at the resonant frequency is  $R_m = 2612 \Omega$  which is very high. To use this structure as an antenna we should match it to  $Z_0 = 50 \Omega$ . An external matching network is not preferred, because it enlarges the overall size of the antenna. In this paper we propose an internal matching mechanism that without size increment, matches the antenna to the desired characteristic impedance.

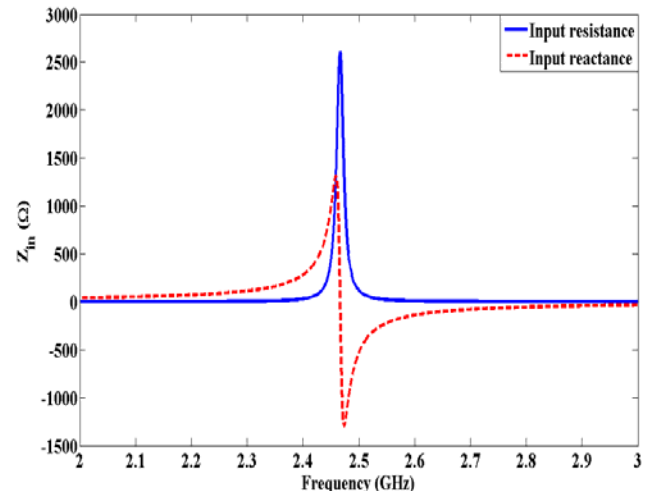


Fig. 4. Input impedance of the one unit cell EZR antenna without capacitive slot ring.

As it can be seen in Fig. 4, there is a specific frequency, below the resonant frequency, at which the input impedance of the resonator is inductive and has a resistance value of  $R = 50 \Omega$ . Hence if we use a series capacitance with proper value, the matching condition at this specific frequency is approximately met. Equating the input impedance of the antenna,  $Z_m$ , with the characteristic impedance of the feed line,  $Z_0 = R_0 = 50 \Omega$ , we can find relations for the new operating angular frequency and the required input series capacitance as follows

$$\omega_1 = \sqrt{\omega_0^2 + \frac{G(1/R_0 - G)}{4C_R^2}} - \frac{1}{2C_R} \sqrt{G(1/R_0 - G)} \quad (2)$$

$$C_m = \frac{1}{\omega_1} \frac{G^2 + \left(\frac{C_R}{\omega_1}\right)^2 (\omega_1^2 - \omega_0^2)^2}{\frac{C_R}{\omega_1} (\omega_0^2 - \omega_1^2)} \quad (3)$$

We use a capacitive slot ring around the feed point to realize the desired series capacitance. The radius of this ring should be adjusted in order that matching condition is met [18].

### 2.4 Simulation and Experimental Results

Figure 5 demonstrates the fabricated antenna as well as its measured, full-wave simulated and circuit simulated  $S_{11}$  parameter. Full-wave and circuit simulation results are obtained using HFSS and ADS, respectively. The equivalent circuit parameters of the antenna used in ADS simulation are  $L_R = 2.57$  nH,  $L_L = 1.12$  nH,  $G = 0.31$  mS,  $C_R = 3.81$  pF and  $C_m = 0.16$  pF. These parameters are extracted using the method presented in [19]. The operating frequency and -10 dB bandwidth of the antenna are 2.39 GHz and 0.4% in simulation and 2.37 GHz and 0.5% in measurement.

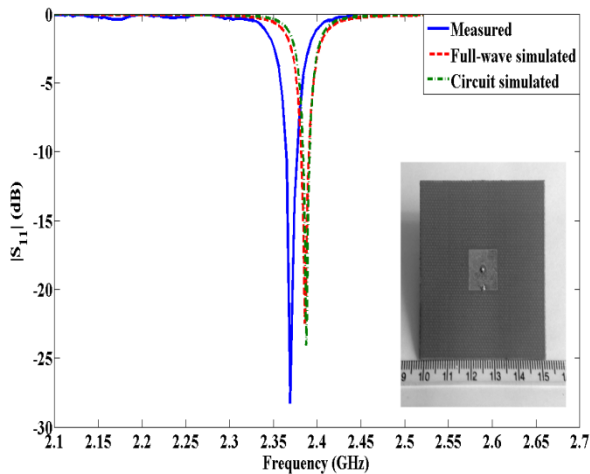


Fig. 5. Photograph of the one unit cell EZR antenna and its  $S_{11}$  parameter.

According to [20], an electrically small antenna, is the antenna which satisfies the condition of  $ka < 1$ . In this condition,  $a$  is the radius of a sphere that surrounds the antenna and  $k$  is the wave number in the free space. For the presented antenna,  $a$  and  $k$  are equal to 8.7 mm and 50.3 rad/m, respectively, and hence  $ka = 0.44$ . In the other words this antenna can be considered as an electrically small antenna.

Figure 6 shows the surface current on the patch. As noted before, this surface current is mainly x-directed. Figure 7 shows the electric field beneath the patch and also magnitude of this field at the edges of the patch. The curves in Fig. 7(b) are plotted with the assumption that the patch centre is on the origin of the coordinate system. According to Fig. 7 the radiated fields due to the equivalent magnetic current at the edges placed at  $y=6.1$  mm and  $y=-6.1$  mm cancel each other at  $xz$  plane and produce cross polarization at  $yz$  plane. The equivalent magnetic current at the  $x=-6.1$  mm and  $x=6.1$  mm edges are not equal, so their radiated

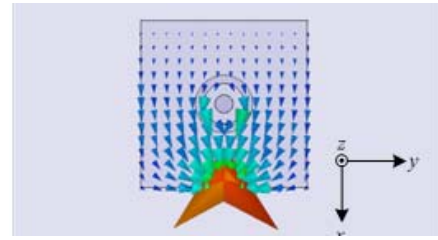


Fig. 6. Surface current on the patch.

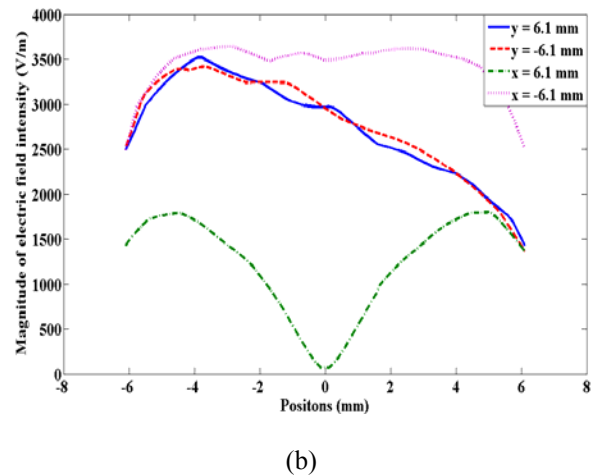
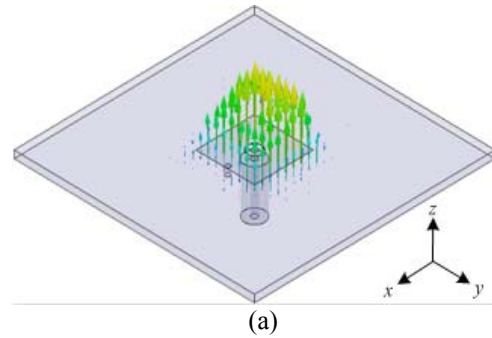


Fig. 7. (a) Electric field beneath the patch (b) magnitude of the electric field at the edges of the patch.

fields do not cancel each other and consequently, they produce a broadside radiation pattern.

In Fig. 8 the measured and simulated radiation patterns of the antenna are shown. Radiation pattern of the antenna is broadside. The higher level of the measured cross polarization component in  $xz$  plane, in comparison with the simulated one, is due to the high cross polarization level of the reference antenna in measurement. The simulated and measured antenna maximum gain are 1.3 dBi and 1.1 dBi, respectively, and the simulated antenna efficiency is 54%. As mentioned before, the radiation of the antenna mainly results from the equivalent magnetic current at  $x=-6.1$  mm and thus this antenna is equivalent to a magnetic dipole antenna. Theoretically, directivity of a dipole antenna near an infinite ground plane is 4.77 dB. With consideration of the antenna efficiency, there is a relatively good agreement between the actual gain and the corresponding theoretical value.

The overall performance of the proposed one unit cell EZR antenna is compared with a few of the previously reported metamaterial antennas in Table 1. The compactness of the presented antenna is evident from this comparison.

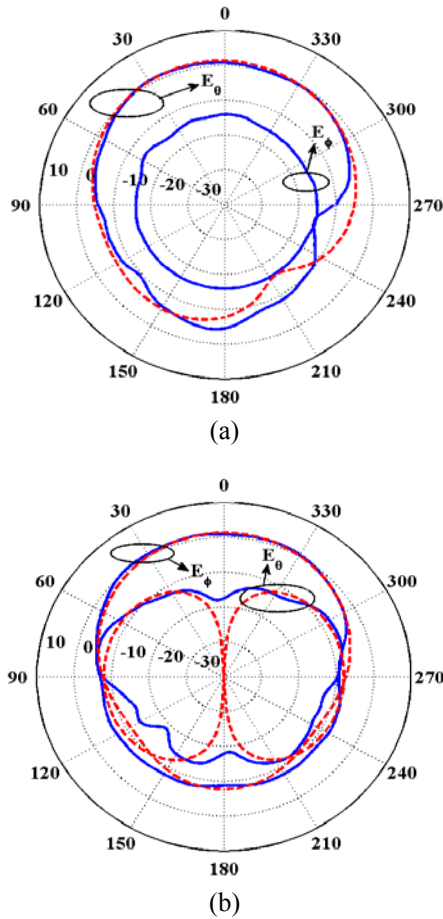


Fig. 8. Measured (solid line) and simulated (dashed line) radiation pattern of the one unit cell EZR antenna (a) xz plane (b) yz plane.

Table 1. Comparison between the performance of the proposed one unit cell EZR antenna and some of the previously reported metamaterial antennas.

	This work	[8]	[9]	[10]	[13]	[21]
Frequency (GHz)	2.37	3.38	6.25	2.03	2.7	3.3
Size	$0.098\lambda_0 \times 0.098\lambda_0$	$0.167\lambda_0 \times 0.167\lambda_0$	$0.108\lambda_0 \times 0.188\lambda_0$	$0.17\lambda_0 \times 0.10\lambda_0$	$0.19\lambda_0 \times 0.13\lambda_0$	$0.250\lambda_0 \times 0.143\lambda_0$
-10 dB fractional BW (%)	0.55	0.1	1.2	6.8	0.6	3.1
Maximum gain (dBi)	1.1	0.87	1.8	1.35	1.22	0.79

### 3. Nine Unit Cell EZR Antenna

Based on the ZORs theory, we noted that the resonant frequency of an EZR antenna is independent of the antenna length and according to (1) this resonant frequency is determined using the equivalent circuit elements. Thus using more unit cells leads to higher gain without change in resonant frequency of the antenna. On this basis we designed and fabricated a nine unit cell EZR antenna. This antenna is shown in Fig. 9. The unit cells of this antenna are the same as the previous one. In order to match this antenna we don't use the capacitive slot ring and only we shift the feed point toward the via holes. In fact, because of using more unit cells in this antenna, the input resistance is reduced to the extent that there is no need to input capacitance for impedance matching.

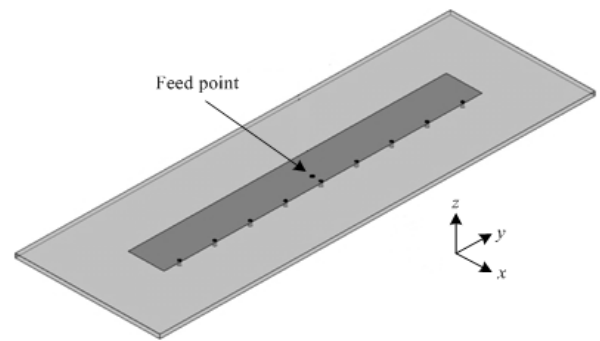


Fig. 9. The proposed nine unit cell EZR antenna.

Figure 10 illustrates the equivalent circuit of the proposed antenna. The inductance of  $L_f$  in middle unit cell of this circuit results from feed point shift. According to this figure and by assuming that  $G$  and  $L_f$  are negligible, there is no current in the series inductances at the zero order resonant frequency and thus, similar to the previous antenna, the current flow on this antenna at the operating frequency is only in the x-direction.

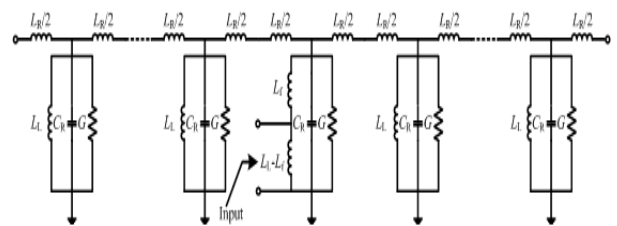


Fig. 10. Equivalent circuit of the proposed nine unit cell EZR antenna.

Figure 11 demonstrates the fabricated antenna as well as its measured, full-wave simulated and circuit simulated  $S_{11}$  parameter. The equivalent circuit parameters of the antenna used in ADS simulation are  $L_R = 1.88$  nH,  $L_L = 1.38$  nH,  $G = 0.75$  mS,  $C_R = 2.97$  pF and  $L_f = 0.5$  nH which are extracted using the method presented in [19]. The operating frequency and -10 dB bandwidth of the antenna are 2.49 GHz and 1.2% in simulation and 2.41 GHz and 1.1% in measurement. There is 3.3% error between the measured and simulated operating frequencies which could be due to

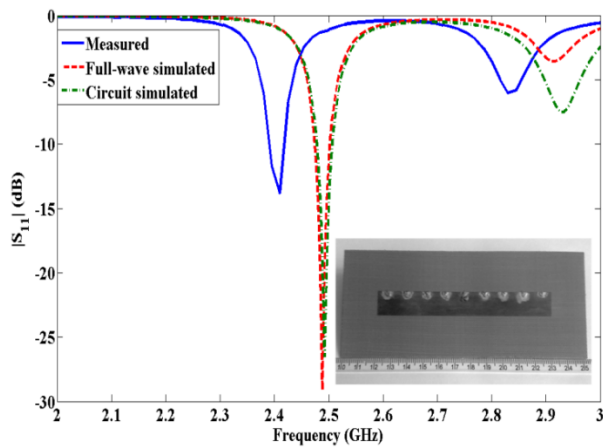
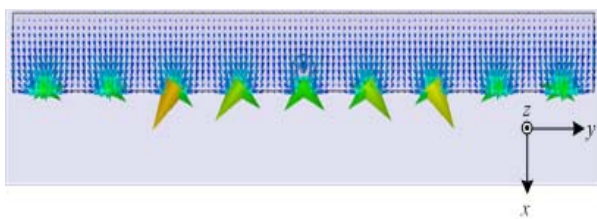


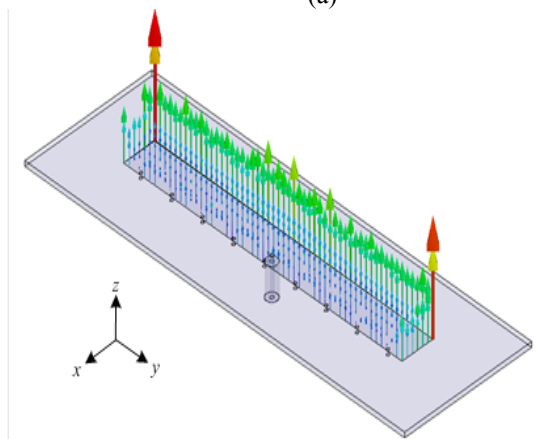
Fig. 11. Photograph of the nine unit cell EZR antenna and its  $S_{11}$  parameter.

the inaccuracy in via holes implementation. Note that the resonance around 2.9 GHz is related to the second order resonant frequency. In fact due to the feed point position, the first order resonant frequency is not excited in the antenna. Although the length of this antenna is nine times the previous one, their resonant frequencies are only a little different from each other.

Figure 12(a) shows the surface current on the patch. Similar to the previous antenna, the surface current on this antenna is mainly x-directed. Figure 12(b) shows the electric field beneath the patch which is in-phase along the antenna as expected. Length of the equivalent magnetic current which results from this in-phase electric field is larger compared with the previous one and this leads to a higher directivity.



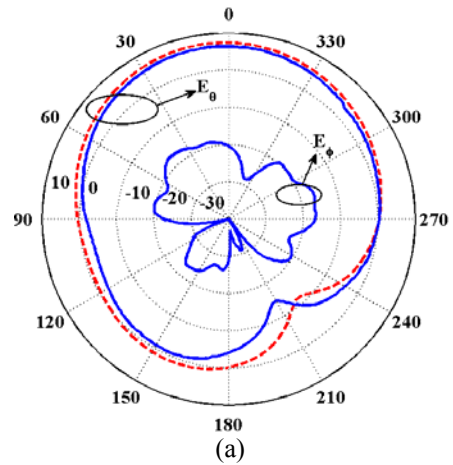
(a)



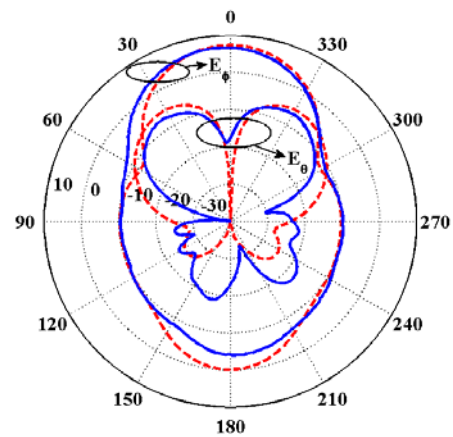
(b)

Fig. 12. (a) Surface current on the nine cell EZR antenna and (b) electric field beneath this antenna.

Figure 13 shows the measured and simulated radiation pattern of this antenna. The simulated and measured antenna maximum gain are 7.3 dBi and 6.4 dBi, respectively, and the simulated antenna efficiency is 86%. The measured gain value of this antenna is 5.3 dB higher than that of the one unit cell antenna.



(a)



(b)

Fig. 13. Measured (solid line) and simulated (dashed line) radiation pattern of the nine unit cell antenna (a) xz plane (b) yz plane.

In general the presented nine unit cell antenna can be considered as a magnetic dipole antenna with uniform current and length of 109.8 mm. Theoretically the directivity of this antenna in vicinity of an infinite ground plane is 4.57 (6.6 dB). Hence, with consideration of the efficiency, the actual gain of this antenna is comparable with the corresponding theoretical value.

From other point of view, the operation of nine unit cell antenna is similar to the Franklin antenna [22]. The Franklin antenna consists of an array of dipoles connected end-to-end by  $\pi$  radians phase-shifting sections. Hence the current distribution on this antenna is co-phased and this leads to a broadside radiation pattern perpendicular to the antenna axis. Similarly the presented nine cell antenna in this section, which is realized using ZOR and modified mushroom-like structure, can be considered as an array of in-phase magnetic dipoles which provides a broadside radiation pattern.



#### 4. Conclusion

In this paper new EZR antennas with broadside radiation pattern were proposed. The previously presented EZR antennas in the literature which use mushroom-like ENG unit cells have monopolar pattern. We used a modified mushroom-like structure which results in broadside radiation pattern. In addition this enhanced ENG unit cell has more compact size compared to the conventional ones. A one unit cell antenna using this configuration was designed and fabricated. Size of this antenna is  $0.098\lambda_0 \times 0.098\lambda_0$  and its operating frequency and maximum gain are  $f_0 = 2.37$  GHz and  $G = 1.1$  dBi, respectively. As shown, this antenna satisfies the condition of  $ka < 1$  and thus it can be considered as an electrically small antenna. The resonant frequency of the ZOR antennas is independent of the antenna length. Thus we designed and fabricated another antenna with nine unit cells of the same structure. The operating frequency of this antenna is  $f_0 = 2.41$  GHz and its maximum gain is 5.53 dB greater than that of the one unit cell antenna. In general the operating frequency and radiation characteristics of the proposed antennas were described with the aid of equivalent circuit model of ENG TLs and theory of ZORs. This description provides a good insight into the behaviour of the presented antennas.

#### Acknowledgment

The authors would like to thank the Research Institute for ICT for financial support of this work.

#### References

- [1] A.K. Iyer, G.V. Eleftheriades, "Negative refractive index metamaterials supporting 2-D waves," in *IEEE-MTT International Microwave Symposium Digest*, vol. 2, Seattle, June 2002, pp. 1067–1070.
- [2] A.A. Oliner, "A periodic-structure negative-refractive-index medium without resonant elements," in *URSI Digest, IEEE-AP-S USNC/URSI National Radio Science Meeting*, San Antonio, June 2002, pp. 41.
- [3] C. Caloz and T. Itoh, "Application of the transmission line theory of left-handed (LH) materials to the realization of a microstrip LH transmission line," in *Proceedings of the IEEE Antennas and Propagation Society International Symposium*, vol. 2, San Antonio, TX, June 2002, pp. 12–415.
- [4] A. Sanada, C. Caloz, and T. Itoh, "Novel zeroth-order resonance in composite right/left handed transmission line resonators," in *Asia-Pacific Microwave Conference*, vol. 3, Seoul, Nov. 2003, pp. 1588–1592.
- [5] A. Sanada, K. Murakami, I. Awai, H. Kubo, C. Caloz, and T. Itoh, "A planar zeroth order resonator antenna using a left-handed transmission line," in *34th European Microwave Conference*, Amsterdam, Oct. 2004, pp. 1341-1344.
- [6] G.V. Eleftheriades, A. Grbic and M. Antoniades, "Negative-refractive-index transmission-line metamaterials and enabling electromagnetic applications," in *IEEE Antennas and Propagation Society International Symposium*, Monterey, CA, June 2004, pp. 1399-1402.
- [7] J.H. Park, Y.H. Ryu, J.G. Lee and J.H. Lee, "Epsilon negative zeroth-order resonator antenna," *IEEE Transactions on Antennas and Propagation*, vol. 55, pp. 3710-3712, 2007.
- [8] A. Lai, K.M.K.H. Leong and T. Itoh, "Infinite wavelength resonant antennas with monopolar radiation pattern based on periodic structures," *IEEE Transactions on Antennas and Propagation*, vol. 55, pp. 868-876, 2007.
- [9] J.H. Park, Y.H. Ryu and J. H. Lee, "Mu-zero resonance antenna," *IEEE Transactions on Antennas and Propagation*, vol. 58, pp. 1865-1875, 2010.
- [10] T. Jang and J. Choi, and S. Lim, "Compact coplanar waveguide (CPW)-fed zeroth-order resonant antennas with extended bandwidth and high efficiency on viiless single layer," *IEEE Transactions on Antennas and Propagation*, vol. 59, pp. 363-372, 2011.
- [11] J. G. Lee and J. H. Lee, "Zeroth order resonance loop antenna," *IEEE Transactions on Antennas and Propagation*, vol. 55, pp. 994-997, 2007.
- [12] A. Rennings, T. Liebig, C. Caloz and P. Waldow, "MIM CRLH series mode zeroth order resonant antenna (ZORA) implemented in LTCC technology," in *Asia-Pacific Microwave Conference*, Dec. 2007, pp. 1–4.
- [13] T.G. Kim and B. Lee, "Metamaterial-based compact zeroth-order resonant antenna," *Electronics Letters*, vol. 45, pp. 12-13, 2009.
- [14] S. Pyo, S. M. Han, J. W. Baik and Y. S. Kim, "A slot-loaded composite right/left-handed transmission line for a zeroth-order resonant antenna with improved efficiency," *IEEE Transactions on Microwave Theory and Techniques*, vol. 57, pp. 2775-2782, 2009.
- [15] W. C. Chang and B. Lee, "Wideband one-unit-cell ENG zeroth-order resonant antenna," *Electronics Letters*, vol. 45, pp. 1289-1291, 2009.
- [16] J. Kim, G. Kim, W. Seong and J. Choi, "A tunable internal antenna with an epsilon negative zeroth order resonator for DVB-H Service," *IEEE Transactions on Antennas and Propagation*, vol. 57, pp. 14014-4017, 2009.
- [17] S. W. Lee and J. H. Lee, "Electrically small MNG ZOR antenna with multi-layered conductor," *IEEE Antennas and Wireless Propagation Letters*, vol. 9, pp. 724-72, 2010.
- [18] M. S. Majedi and A. R. Attari, "A compact mu negative zeroth order resonator antenna," *Metamaterials*, vol. 6, pp. 64-69, 2012.
- [19] T. Liebig, S. Held, A. Rennings and D. Erni, "Accurate parameter extraction of lossy composite right/left-handed (CRLH) transmission lines for planar antenna applications," in *Fourth International Congress on Advanced Electromagnetic Materials in Microwaves and Optics*, 2010.
- [20] W. L. Stutzman and G. A. Thiel, *Antenna Theory and Design*, New York: John Wiley & Sons, 1981.
- [21] J. Zhu and G. V. Eleftheriades, "A compact transmission-line metamaterial antenna with extended bandwidth," *IEEE Antennas and Wireless Propagation Letters*, vol. 8, pp. 295–298, 2009.
- [22] H. Jasik, *Antenna Engineering Handbook*, 1st ed., New York: Mc-Graw-Hill, 1961.



**Mohammad Saeed Majedi** was born in Shiraz, Iran, on May 7, 1983. He received the B.Sc. degree in electrical engineering from the Ferdowsi University of Mashhad, Mashhad, Iran, in 2006, the M.Sc. degree in electrical engineering from the Sharif University of Technology, Tehran, Iran in

2008 and Ph.D. degree in electrical engineering from Ferdowsi University of Mashhad in 2013.

In 2013, he joined the Department of Electrical Engineering, Ferdowsi University of Mashhad, where he is currently an assistant professor. His research interests include microwave circuit design, wave propagation, metamaterials and antenna design.



**Amir Reza Attari** was born in Mashhad, Iran, on September 20, 1971. He received his B.S. and M.S. degrees in electrical engineering from the Sharif University of Technology, Tehran, Iran, in 1994 and 1996, respectively. He received his Ph.D. degree in electrical engineering jointly from the

Sharif University of Technology, Tehran, Iran, and University of Joseph Fourier, Grenoble, France, in 2002.

In 2004, he joined the Department of Electrical Engineering, Ferdowsi University of Mashhad, where he is currently an associate professor. His research interests are antennas, passive microwave devices and numerical methods in electromagnetic.

